Electromagnetic component of $10^{14}-10^{16}$-eV air showers

E. J. Fenyves, S. N. Balog, N. R. Davis, and D. J. Suson
University of Texas at Dallas, Richardson, Texas 75083-0688

Todor Stanev
Bartol Research Institute, University of Delaware, Newark, Delaware 19716
(Received 3 August 1987)

Detailed Monte Carlo simulations of the electromagnetic component of extensive air showers generated by $10^{14}-10^{16}$-eV protons and iron nuclei have been carried out. The longitudinal development and lateral distribution of the electron component was approximated with parametrized analytical formulas, and compared for proton- and iron-initiated extensive air showers.

I. INTRODUCTION

Interest in air-shower studies has been recently revived, mostly because of observations of point sources of high-energy cosmic γ rays. New large air-shower arrays are in the design or construction stage which will have qualitative advantages over similar devices of the past. An increased sensitive area, precise simultaneous measurement of several shower components, and vastly improved electronics, all design features of the new detectors, will enhance their ability to measure particle fluxes and derive the shower parameters.

In addition to the search for point sources of cosmic γ rays and other signals from sites of cosmic-ray acceleration, these detectors will be efficient in answering in detail the classical astrophysical questions of the energy spectrum and the nuclear composition of the cosmic rays at $10^{14}-10^{16}$ eV. This energy range is of specific interest because (1) it includes the region of drastic changes of the energy spectrum, related to the acceleration processes and the structure of the Galaxy, and (2) its lower edge provides an overlap with direct satellite and balloon measurements.

Independent of the improved measurements, the new experiments will still require detailed Monte Carlo simulations of the shower development as a basis of the data analysis and interpretation. These calculations should (a) show the differences of the basic parameters for showers initiated by various primary particles, and (b) help with the design of the arrays and the determination of the shower parameters.

Our calculations are specifically aimed at aiding the data analysis of the Homestake surface-underground telescope,[1-3] but because they deal with the most basic parameters of the shower size, longitudinal development, and lateral distribution, they can be applied to any shower detector located at sea-level or mountain altitudes. The surface array of the Homestake experiment measures the electron densities, reconstructs the location of the shower core and the electron lateral distribution, and uses them to derive the total number of electrons N_e. The underground detector measures the number N_μ, the direction, and the lateral spread of the penetrating muons. The shower size N_e gives the estimate of the primary energy, and the correlation with N_μ and other characteristics of the muons is used to derive the nuclear composition of the primary flux. The lateral spread of the muons can also be used to study some features of the forward region of the interaction of the primary nucleons with the air nuclei of the atmosphere, which is hardly accessible for colliders.

In this paper we report on the results obtained for the electromagnetic component of extensive air showers generated by $10^{14}-10^{16}$-eV protons and iron nuclei. We give parametrizations of the longitudinal and lateral development of the shower. We also give the average number of muons ($E_\mu > 1.7$ TeV) produced in such showers, which allows an estimate of the ability of the surface-underground-telescope to study the primary-cosmic-ray composition.

II. SIMULATION OF THE ELECTROMAGNETIC CASCADES

Monte Carlo simulations of electron-photon cascades generated by primary photons and electrons of 0.1-, 1.0-, and 10-TeV energy have been carried out using the program developed by Stanev and Vankov.[4] This program includes the processes of the bremsstrahlung, pair production, Compton effect, and multiple Coulomb scattering. The bremsstrahlung and pair-production routines account for appropriate screening of the nucleus.[5] The ionization loss is calculated along the electron path length using the Bethe-Bloch formula.[6] The electrons are followed to a threshold energy of 5, 10, 15, or 20 MeV in order to simulate showers detected by different experimental arrangements having electron detectors of different threshold energies.

We have run a total of 4000 electron-photon showers generated by 0.1-, 1.0-, and 10-TeV photons and electrons at $t = 2,4,\ldots,20$ radiation lengths above the Homestake surface detector (850 g/cm^2), and above sea

 ©1988 The American Physical Society

level in a standard atmosphere. The longitudinal development of photon- or electron-induced electromagnetic cascades fits reasonably well with a modified form of the formula introduced first by Greisen[7] and used by Hillas[8] in Monte Carlo simulation of 0.1-TeV-photon–induced showers

$$N_e(E_0,E,t)=\frac{\alpha A(E)0.31}{\sqrt{y}}\exp[t_1(1-1.5\ln s_1)] , \quad (1)$$

where N_e is the number of electrons, E_0 is the energy of the primary photon or electron, t is the depth measured in radiation lengths (37.1 g/cm^2 in air), and E the threshold energy of electrons.[9] α is the number of primary particles (photons or electrons) generating the shower, and is obviously equal to 1 for the above case. $A(E)$ is the fraction of electrons having energies larger than E as compared to the total number of electrons, and $y=\ln E_0/\epsilon_0$ with $\epsilon_0=81$ MeV for air. t_1 is the modified depth

$$t_1=t+a_{\pi,\gamma}(E) , \quad (2)$$

with $a_\pi(E)$ and $a_\gamma(E)$ accounting for the different development and different $t_{\max}$ values of electron- and photon-induced showers, respectively, with different electron threshold energies. The modified age parameter s_1 is calculated with the modified t_1 value as

$$s_1=\frac{3t_1}{t_1+2y} . \quad (3)$$

Tabulated values of $A(E)$, $a_\pi(E)$, and $a_\gamma(E)$ for different threshold energies E are given in Table I. The $A(E)$ values, as well as the $a_\pi(E)$, $a_\gamma(E)$, $b_\pi(E)$, and $b_\gamma(E)$ values, can be interpolated for intermediate E values with a reasonable accuracy when plotted on a log-log or lin-log scale versus E, respectively. [The parameters b_π and b_γ are defined in Eq. (6).]

A comparison of the longitudinal development of Monte Carlo–simulated electromagnetic cascades above 850 g/cm^2 and at sea level in a standard atmosphere showed for equal t values smaller fluctuations in N_e than the statistical errors of the simulation. Therefore the 850-g/cm^2- and sea-level-based simulations were combined.

Figures 1 and 2 show the results obtained for photon- and electron-induced showers with $E=5$ MeV threshold energy for electrons. The smooth curves were calculated using $A(E)=0.67$, the best-fit value (see Table I), which

TABLE I. Constants for the parametrization of electromagnetic cascades.

	$E=5$ MeV	10 MeV	15 MeV	20 MeV
$A(E)$	0.67	0.59	0.52	0.48
$a_\pi(E)$	0.6	0.8	0.92	1.0
$a_\gamma(E)$	0	0.2	0.32	0.4
$b_\pi(E)$	0.2	0.4	0.52	0.6
$b_\gamma(E)$	−0.4	−0.2	−0.08	0

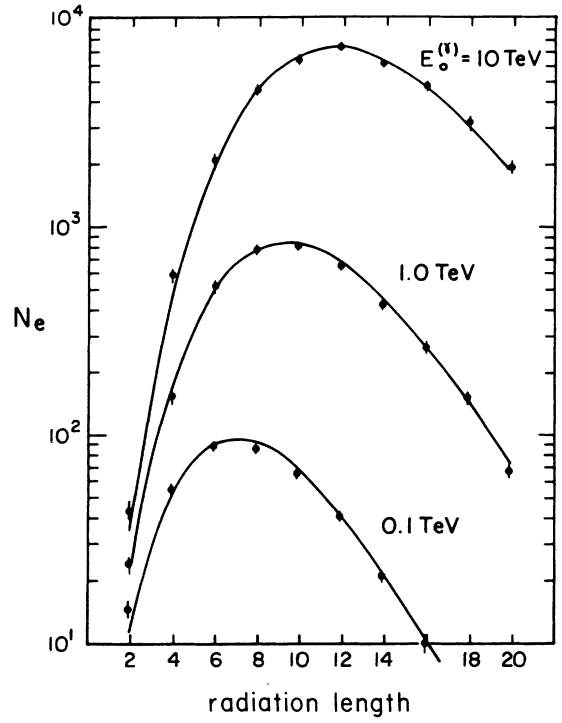

FIG. 1. Longitudinal development of the electron component of photon-initiated electromagnetic showers with $E=5$ MeV electron threshold energy.

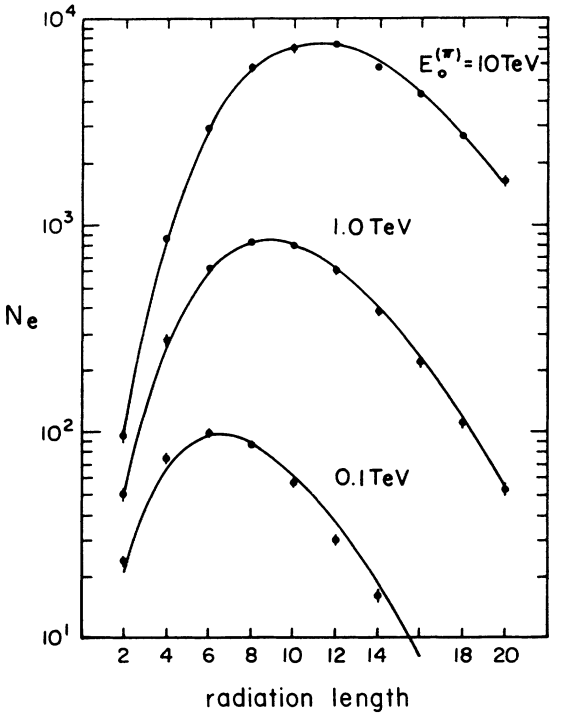

FIG. 2. Longitudinal development of the electron component of electron-initiated electromagnetic showers with $E=5$ MeV electron threshold energy.

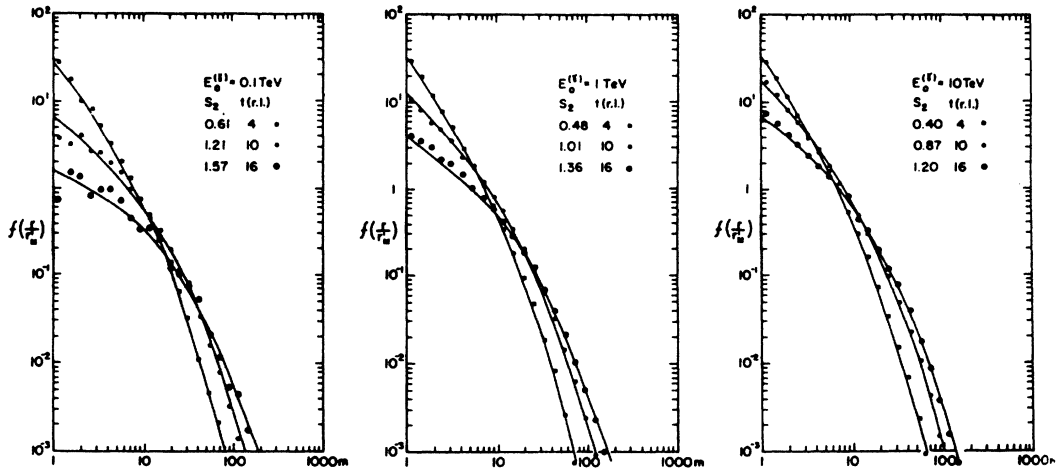

FIG. 3. Lateral distribution of the electron component of photon-initiated electromagnetic showers with $E=5$ MeV electron threshold energy at 850 g/cm^2.

is also equal to the value calculated by Nishimura[10] for the shower maximum using the exact cascade shower solutions in approximation B first obtained by Snyder,[11] Serber,[12] and Scott.[13] The N_e values calculated with Eq. (1) are slightly deviating from the Monte Carlo–simulated values at small and large depths [$t\sim 2$ radiation lengths (r.l.) and $t\sim 20$ r.l.], probably because of using s-independent $A(E)$ values. Similar results were obtained for other threshold energies ($E=10$, 15, and 20 MeV).

The best fit was obtained with $a_\pi(E)-a_\gamma(E)=0.6$ radiation length for all E values, which leads to a 0.6 radiation length difference in the $t_{\max}$ values of electron- and photon-initiated showers as expected theoretically.[10]

The lateral distributions of electrons simulated from $r=1$ to 1000 m agree well with a modified form of the Nishimura-Kamata-Greisen (NKG) formula[7]

$$f\left[\frac{r}{r'_M},s_2,E\right]=C(s_2)\left[\frac{r}{r'_M}\right]^{s_2-2}\left[\frac{r}{r'_M}+1\right]^{s_2-4.5}, \quad (4)$$

where r'_M is about one-half of the Molière length r_M, as suggested by Hillas,[14] and

$$s_2=\frac{3t_2}{t_2+2y} \quad (5)$$

with

$$t_2=t+b_{\pi,\gamma}(E)\,, \quad (6)$$

where $b_\pi(E)$ and $b_\gamma(E)$ are again accounting for the different development and aging of electron- and photon-initiated showers with different electron threshold energies. The best fit was obtained with $r'_M=45$ m

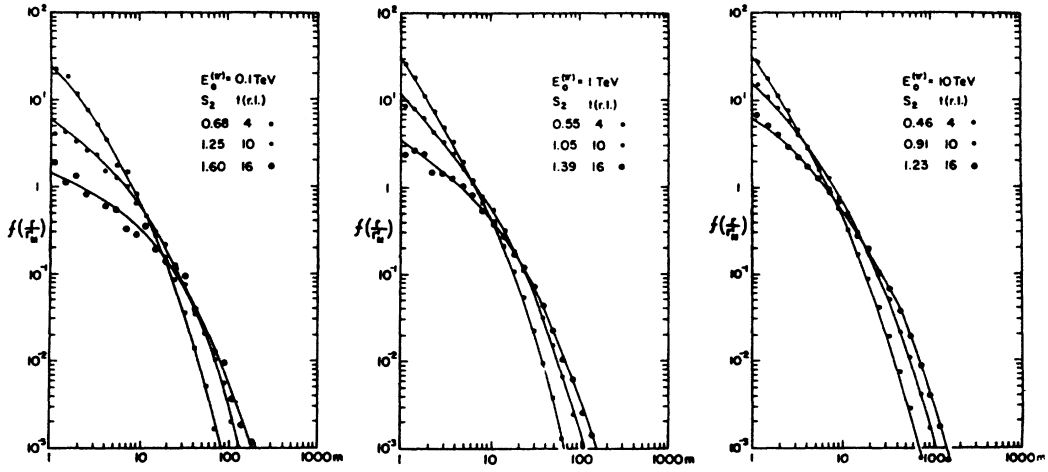

FIG. 4. Lateral distribution of the electron component of electron-initiated electromagnetic showers with $E=5$ MeV electron threshold energy at 850 g/cm^2.

TABLE II. The average number of γ's and electrons per shower above the corresponding threshold energies, and the average number of muons per shower above 1.7 TeV for proton-initiated air showers.

E_p (eV)	N_γ	N_e	N_μ
10^{14}	361±8	3.9±0.3	0.30±0.06
10^{15}	2612±61	31.9±1.1	1.54±0.17
10^{16}	3015±78	34.9±1.2	8.20±0.50

at 850 g/cm^2, and correspondingly with $r'_M=37.5$ m at sea level. The best-fit $b_\pi(E)$ and $b_\gamma(E)$ values are shown in Table I.

Figures 3 and 4 show the lateral distributions of the electron component of 0.1-, 1.0-, and 10-TeV photon- and electron-initiated showers at selected depths for $E=5$-MeV electron threshold energy. The s_2 values are smaller than the s_1 values. Thus the lateral distribution is characterized with a somewhat smaller average age than the longitudinal development of the shower. The electron density Δ can be calculated from the function f by $\Delta=N_e f/r'^2_M$, where N_e is the total number of electrons.

III. SIMULATION OF EXTENSIVE AIR SHOWERS GENERATED BY 10^{14}–10^{16}-eV PROTONS

We have run a total of 220 extensive air showers generated by 10^{14}-, 10^{15}-, and 10^{16}-eV primary protons in a standard atmosphere. The γ's and electrons generated in the hadronic cascades were followed until they reached the following threshold energies: 0.01 TeV for 10^{14}- and 10^{15}-eV primary protons, and 0.1 TeV for 10^{16}-eV protons. The higher threshold value for 10^{16}-eV-proton–initiated showers was chosen in order to keep the number of photons at a reasonable level for further calculations.

The model of the inelastic interactions used in the simulations obeys radial scaling, and at $\sqrt{s}=540$ GeV produces a charged multiplicity of 26 particles, fully compatible with the results of the CERN $\bar{p}p$ collider experiments. The x distribution of the secondaries is realized through the splitting technique, suggested by Hillas,[15] which has the advantage of automatically conserving the interaction energy. The charged K/π ratio has a constant value of 0.09. The proton-air inelastic cross section increases with energy as $\log^{1.8}s$, which corresponds to a $\log^2 s$ law for inelastic pp collisions.[16]

The transverse-momentum distribution is of the form $p_t e^{-Kp_t}$ and includes the "seagull" effect, which is important for the lateral spread of both the electromagnetic cascades generated by high-energy γ's, and the high-energy muons. For $x<0.2$, $K=2/(x+\frac{1}{4})$, while a constant exponent of -4.44 is used for pions. The average transverse momentum for kaons is 0.4 GeV/c and for nucleons is 0.5 GeV/c.

The average number of γ's and electrons per shower above the corresponding threshold energies is shown in Table II. The average number of muons above 1.7 TeV, the threshold energy for a muon to reach the 4200 mwe (meters of water equivalent) deep Homestake detector, is also included in the table.

The electromagnetic cascades generated by γ's and electrons are propagated to the height of detection by applying the parametrized analytical formulas for the longitudinal development and lateral distribution of the electron component presented in Sec. II.

In order to correct the total number of electrons N_e for the missing low-energy electromagnetic cascades generated by photons having energies less than the threshold levels, the γ spectra were extrapolated below the threshold levels and correction factors for N_e were calculated. It turned out that the correction factors which are dependent on the depth and the primary proton energy are very small ($\sim$1–2 %).

The geomagnetic effect was included in the calculation by stretching the east-west axis of each vertical electromagnetic cascade by $[1+0.05(\cos\lambda/P)^2]^{1/2}$, where λ

TABLE III. Constants for the parametrization of proton-initiated air showers.

E_p (eV)	E_0 (eV)	β	γ
10^{14}	5.2×10^{13}	0.0100	1.00
10^{15}	6.4×10^{14}	0.0173	0.75
10^{16}	6.9×10^{15}	0.0300	0.50

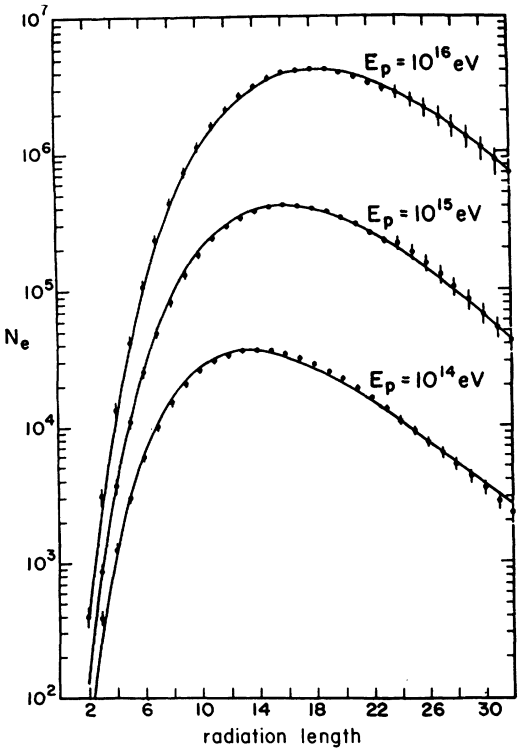

FIG. 5. Longitudinal development of the electron component of extensive air showers generated by 10^{14}–10^{16}-eV protons with $E=5$ MeV electron threshold energy.

is the geomagnetic latitude and P the pressure in atmospheres.[7] The individual cascades were then folded together to form the electron component of the extensive air shower.

The geomagnetic effect is relatively small at sea level but increases with altitude. The east-west axis of vertical extensive air showers is stretched by a factor 1.013 at sea level, and 1.019 at 850 g/cm^2. The relative difference between the $f(r/r'_M)$ values averaged in a cone $\pm 45°$ around the north-south axis is increasing with r but remains very small ($\lesssim 1.5\%$).

As expected the longitudinal development of extensive air showers generated by 10^{14}–10^{16}-eV protons could not be approximated well with Eq. (1), the formula used for electromagnetic cascades generated by γ's or electrons. We could, however, fit the total number of electrons at the shower maximum, $N_e^{\max}$, and the depth of the maximum, $t_{\max}$, calculated from Eq. (1) simultaneously to the corresponding average values obtained for the Monte Carlo–simulated 10^{14}-, 10^{15}-, and 10^{16}-eV showers by assuming a single primary γ ($\alpha = 1$) and varying its energy E_0 (Ref. 17). The longitudinal development of the simulated air showers was, however, increasing faster before $t_{\max}$ and decreasing slower after $t_{\max}$ than the values calculated from Eq. (1). This is expected because the electromagnetic component of the air shower starts with a large number of γ's, and dies out slower after the max-

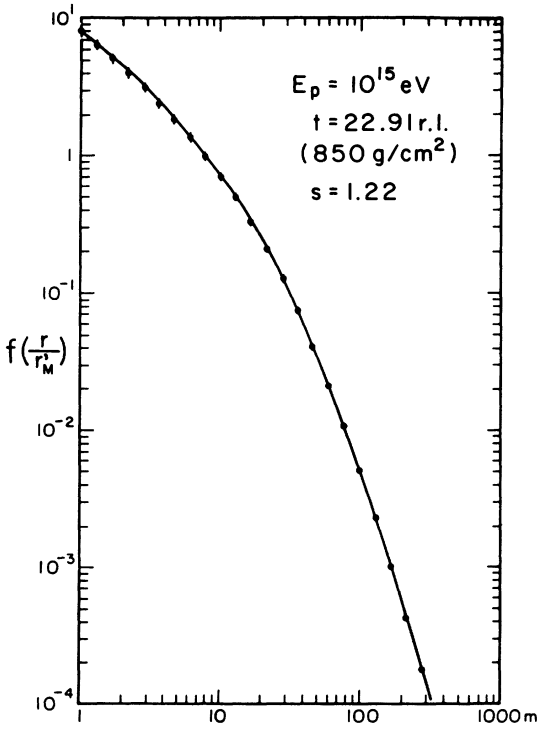

FIG. 7. Lateral distribution of the electron component of extensive air showers generated by 10^{15}-eV protons with $E = 5$ MeV electron threshold energy at 850 g/cm^2.

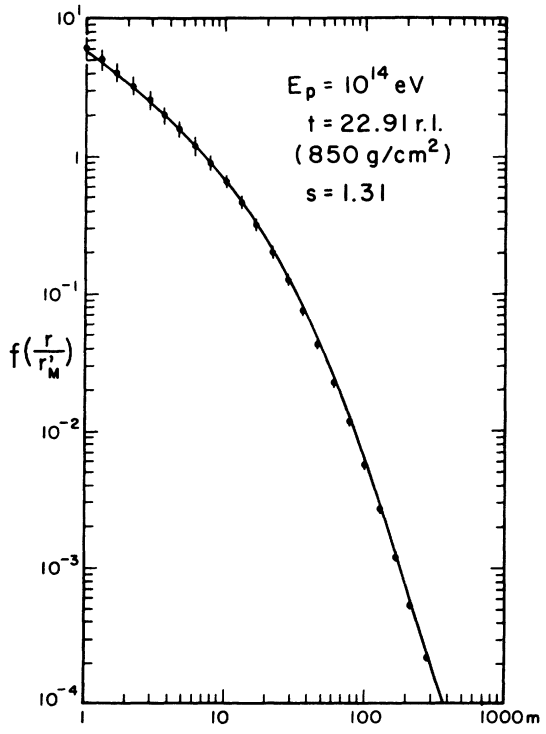

FIG. 6. Lateral distribution of the electron component of extensive air showers generated by 10^{14}-eV protons with $E = 5$ MeV electron threshold energy at 850 g/cm^2. The electron density Δ, can be calculated from f, by $\Delta = N_e f / r'^2_M$, where N_e is the total number of electrons and r'_M is about half of the Molière length ($r'_M = 45$ m at 850 g/cm^2).

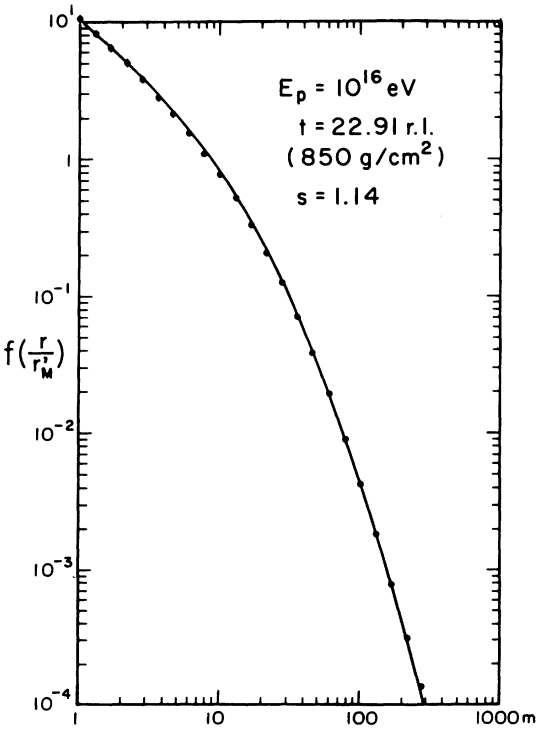

FIG. 8. Lateral distribution of the electron component of extensive air showers generated by 10^{16}-eV protons with $E = 5$ MeV electron threshold energy at 850 g/cm^2.

TABLE IV. The average number of γ's and electrons above the corresponding threshold energies, and the average number of muons per shower above 1.7 TeV for iron-initiated air showers.

E_{Fe} (eV)	N_γ	N_e	N_μ
10^{14}	794±18	6.3±0.8	0
10^{15}	5138±49	62.5±2.3	2.21±0.27
10^{16}	5657±53	61.4±2.2	24.40±0.70

imum due to new electromagnetic cascades generated by the hadronic core.

According to this we modified Eqs. (1) and (3) by replacing t_1 in both equations by

$$t' = t + \beta(t_{max} - t)t^\gamma , \quad (7)$$

where β and γ are constants depending on the primary proton energy, and the second term increases or decreases the effective depth t', as compared to t before or after the maximum, respectively.

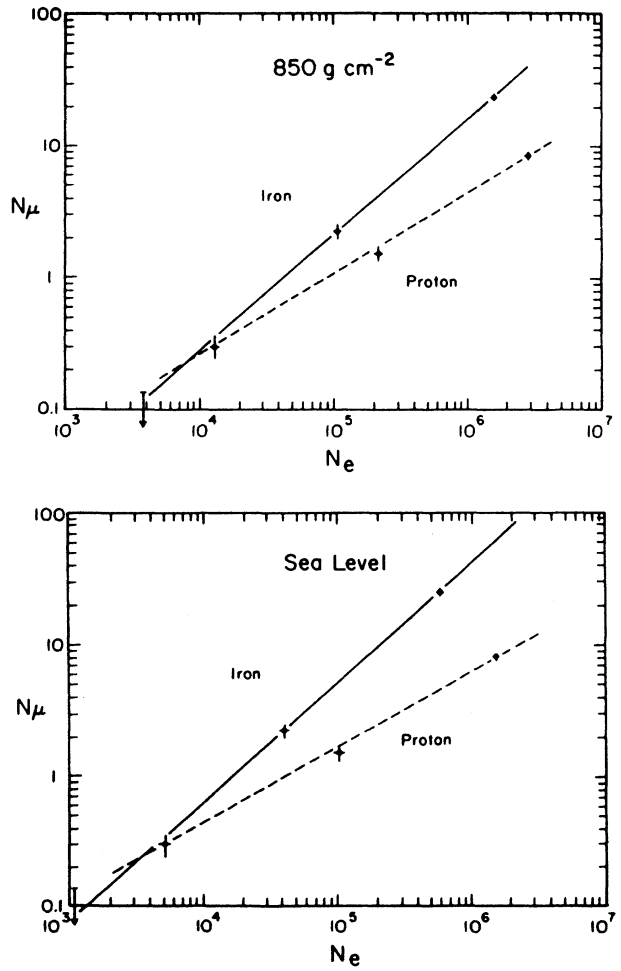

FIG. 9. The total number of electrons detected at 850 g/cm^2 and at sea level versus the total number of penetrating muons ($E_\mu > 1.7$ TeV) for iron- and proton-initiated showers.

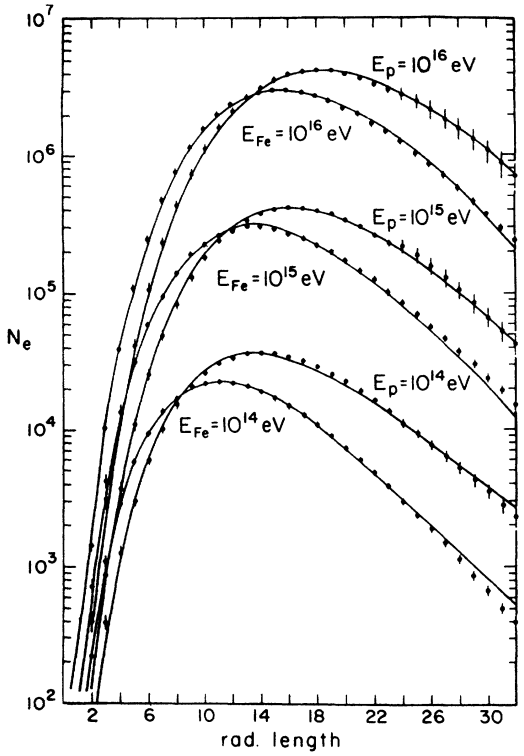

FIG. 10. Longitudinal development of the electron component of extensive air showers generated by 10^{14}–10^{16}-eV iron nuclei with $E = 5$ MeV electron energy compared to that of proton-generated showers.

The optimum E_0, β, and γ values obtained for this parametrization for $E_p = 10^{14}$, 10^{15}, and 10^{16} eV and $E = 5$ MeV are given in Table III. The β and γ values can be easily interpolated for intermediate E_p values when plotted on a log-log or lin-log scale versus E_p, respectively. Figure 5 shows a good agreement between the Monte Carlo–simulated average N_e values (dots with error bars) and the smooth curves calculated by using Eqs. (1) and (3) and replacing t_1 by t' [Eq. (7)]. It was shown that the above equations can be used to describe moderately inclined showers ($\Theta \leq 30°$). Then t in Eq. (7) is the slant depth measured from the top of the atmosphere.

It can be seen from Table III that the relative energy of the single γ, E_0/E_p, simulating the longitudinal development of the air shower, is increasing with E_p, the energy of the primary proton, as expected, because the probability of charged pions and kaons to produce nu-

TABLE V. Constants for the parametrization of iron-initiated air showers.

E_{Fe} (eV)	E_0 (eV)	α	β	γ
10^{14}	4.2×10^{12}	7	0.010	1.00
10^{15}	5.2×10^{13}	8.5	0.0173	0.75
10^{16}	5.2×10^{14}	9	0.030	0.50

clear interactions rather than decay is increasing with energy. Thus at higher energies a larger fraction of the primary proton energy goes into the electromagnetic cascade.

The Monte Carlo–simulated lateral distribution of electrons in extensive air showers generated by 10^{14}-, 10^{15}-, and 10^{16}-eV protons was compared with the modified NKG formula [Eqs. (4) and (5)] and replacing t_2 by t' [Eq. (7)], the effective depth used in the parametrization of the longitudinal development. A good agreement was found for not-too-large distances from the core, for $r=1$ m to about 300 m, both for mountain altitudes (850 g/cm^2) and sea level, as illustrated in Figs. 6–8. At larger distances from the core, however, even the modified NKG formula fails to agree with the Monte Carlo–simulated data. Corrections for this effect will be discussed in a forthcoming paper.

IV. SIMULATION OF EXTENSIVE AIR SHOWERS GENERATED BY 10^{14}–10^{16}-eV IRON NUCLEI

We have run a total of 280 extensive air showers generated by 10^{14}-, 10^{15}-, and 10^{16}-eV primary iron nuclei in a standard atmosphere. The hadronic cascades were simulated using the interaction and fragmentation model.[18] The γ's and electrons generated in the hadronic cascades were again followed until they reached 0.01 TeV for 10^{14}- and 10^{15}-eV primary iron nuclei, and 0.1 TeV for 10^{16}-eV iron nuclei. The average number of γ's and electrons per shower above the corresponding thresholds and the average number of muons above 1.7 TeV are given in Table IV.

The total number of electrons N_e was obtained after making similar small corrections for the missing low-energy electromagnetic cascades as in the case of the proton-generated air showers. The geomagnetic effect turned out to be small, as for the proton-generated showers.

Plotting the total number of electrons, N_e, measured at mountain altitudes and at sea level versus the total number of penetrating muons, N_μ, for both the iron- and proton-generated showers (Fig. 9) shows that one can distinguish between the iron- and proton-generated showers with a good resolution only at $\geq 10^{16}$-eV primary energies.[19]

The longitudinal development of the extensive air showers generated by 10^{14}–10^{16}-eV iron nuclei can be approximated very well with Eq. (1) as shown in Fig. 10 using best-fit values for E_0, α, β, and γ which are different from the corresponding values obtained for proton-generated showers (Table V). The major difference is in the α values, which vary between 7 and 9 for 10^{14}–10^{16}-eV iron nuclei, and in the E_0 values, which are about one order of magnitude smaller than the corresponding values obtained for 10^{14}–10^{16}-eV proton primaries.[19]

This can be interpreted in the following way: In order to simulate iron-generated air showers, one cannot use one single primary γ as in the case of proton-generated air showers, but needs to use an energy-dependent larger number of primary γ's with correspondingly smaller en-

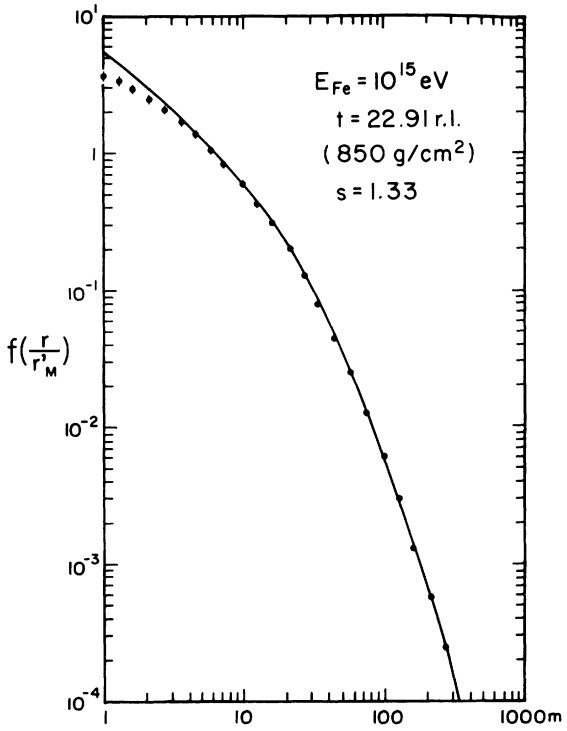

FIG. 11. Lateral distribution of the electron component of extensive air showers generated by 10^{15}-eV iron nuclei with $E=5$ MeV electron threshold energy at 850 g/cm^2.

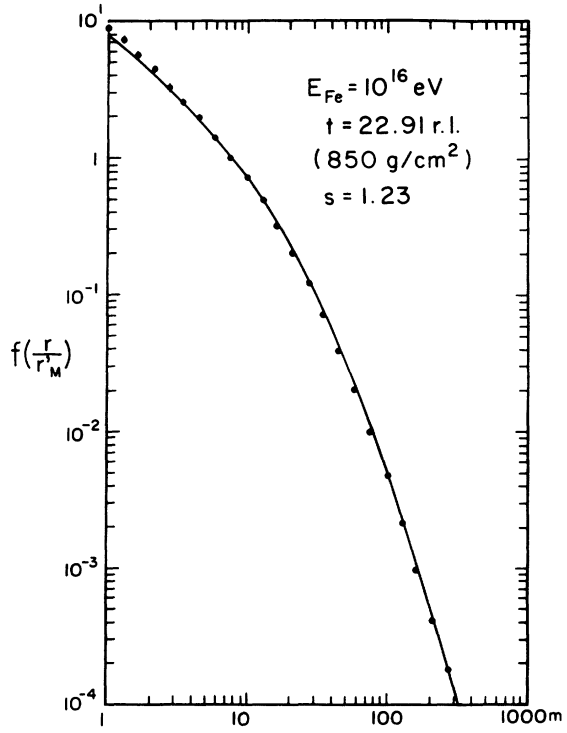

FIG. 12. Lateral distribution of the electron component of extensive air showers generated by 10^{16}-eV iron nuclei with $E=5$ MeV electron threshold energy at 850 g/cm^2.

ergy, due to the fragmentation of the shower-generating iron nucleus and the simultaneous development of a corresponding number of independent hadronic cascades. According to this the iron-generated showers have a steeper increase of N_e before the maximum, smaller $t_{\max}$ and N_e values than the proton showers of the same energy, and N_e is decreasing faster after $t_{\max}$ as compared to the proton showers.

The lateral distribution of electrons can be relatively well approximated with the modified NKG formula [Eqs. (4) and (5)] and replacing t_2 by t' [Eq. (7)] using best-fit values given in Table V for 10^{15}–10^{16}-eV iron-generated air showers, from $r=1$ m to about 300 m (Figs. 11 and 12). For the 10^{14}-eV iron-generated air showers, however, the lateral distribution could not be approximated with this formula. A possible reason is that the threshold energy for γ's and electrons (0.01 TeV) is too high as compared to the energy per nucleon of the primary particles (10^{14} eV/56). Studies are currently carried out to better understand this phenomenon and find another modified formula for these lower-energy showers.

ACKNOWLEDGMENTS

The authors are deeply indebted to T. K. Gaisser, A. M. Hillas, and M. L. Cherry for their valuable comments and helpful discussions, and to E. A. Marshall for her cooperation. This work has been supported by the National Science Foundation under Grants Nos. PHY 8217896 and PHY 8613080.

[1]M. L. Cherry, I. Davidson, K. Lande, C. K. Lee, and R. I. Steinberg, in *Proceedings of the Cosmic Ray Workshop,* Salt Lake City, Utah, 1983, edited by T. Gaisser (Bartol Research Foundation, Newark, Delaware, 1983), p. 164.

[2]M. L. Cherry, S. Corbato, T. Daily, E. J. Fenyves, D. Kieda, K. Lande, and C. K. Lee, in *Proceedings of the 19th International Cosmic Ray Conference,* La Jolla, California, 1985, edited by F. C. Jones, J. Adams, and G. M. Mason (NASA Conf. Publ. 2376) (Goddard Space Flight Center, Greenbelt, MD, 1985), Vol. 8, p. 246.

[3]E. J. Fenyves and M. L. Cherry, in *Proceedings of the Cosmic Ray Workshop,* Salt Lake City, Utah, 1983, edited by T. Gaisser (Bartol Research Foundation, Newark, Delaware, 1983), p. 173.

[4]T. Stanev and Ch. Vankov, Comput. Phys. Commun. **16**, 363 (1979).

[5]B. Rossi, *High Energy Particles* (Prentice-Hall, Englewood Cliffs, NJ, 1952).

[6]H. A. Bethe, Phys. Rev. **89**, 1256 (1953).

[7]K. Greisen, Prog. Cosmic Ray Phys. **3**, 1 (1956).

[8]A. M. Hillas, J. Phys. G **8**, 1461 (1982).

[9]E. J. Fenyves, C. J. Lee, and B. C. Yunn, in *18th International Cosmic Ray Conference, Bangalore, India, 1983, Conference Papers,* edited by N. Durgaprasad (Tata Institute of Fundamental Physics, Bombay, 1983), Vol. 11, p. 240.

[10]J. Nishimura, Handbook of Physics (Springer, Berlin, 1967), Vol. 46/2, p. 1.

[11]H. S. Snyder, Phys. Rev. **53**, 960 (1938); **76**, 1563 (1949).

[12]R. Serber, Phys. Rev. **54**, 317 (1938).

[13]W. T. Scott, Phys. Rev. **80**, 611 (1950).

[14]A. M. Hillas (private communication).

[15]A. M. Hillas, in *Proceedings of the 17th International Cosmic Ray Conference,* Paris, France, 1981 (CEN, Saclay, 1981).

[16]T. K. Gaisser and G. B. Yodh, Annu. Rev. Nucl. Part. Sci. **30**, 475 (1980).

[17]E. J. Fenyves, B. C. Yunn, and T. Stanev, in *Proceedings of the 19th International Cosmic Ray Conference* (Ref. 2), Vol. 8, p. 246.

[18]The fragmentation model is based on the experimental data as described in T. K. Gaisser, T. Stanev, P. Freier, and C. J. Waddington, Phys. Rev. D **25**, 2341 (1982).

[19]E. J. Fenyves, N. R. Davis, D. J. Suson, and Todor Stanev, 10th European Cosmic Ray Symposium, Bordeaux, France, 1986 (unpublished).